RESEARCH ARTICLE

Coaxial Electrohydrodynamic Bioprinting of Pre-vascularized Cell-laden Constructs for Tissue Engineering

Mao Mao[1,2], Hongtao Liang[1,2], Jiankang He[1,2]*, Ayiguli Kasimu[1,2], Yanning Zhang[1,2], Ling Wang[1,2], Xiao Li[1,2], Dichen Li[1,2]

[1]State Key Laboratory for Manufacturing Systems Engineering, Xi'an Jiaotong University, Xi'an 710049, China
[2]NMPA Key Laboratory for Research and Evaluation of Additive Manufacturing Medical Devices, Xi'an Jiaotong University, Xi'an 710049, China

Abstract: Recapitulating the vascular networks that maintain the delivery of nutrition, oxygen, and byproducts for the living cells within the three-dimensional (3D) tissue constructs is a challenging issue in the tissue-engineering area. Here, a novel coaxial electrohydrodynamic (EHD) bioprinting strategy is presented to fabricate thick pre-vascularized cell-laden constructs. The alginate and collagen/calcium chloride solution were utilized as the outer-layer and inner-layer bioink, respectively, in the coaxial printing nozzle to produce the core-sheath hydrogel filaments. The effect of process parameters (the feeding rate of alginate and collagen and the moving speed of the printing stage) on the size of core and sheath lines within the printed filaments was investigated. The core-sheath filaments were printed in the predefined pattern to fabricate lattice hydrogel with perfusable lumen structures. Endothelialized lumen structures were fabricated by culturing the core-sheath filaments with endothelial cells laden in the core collagen hydrogel. Multilayer core-sheath filaments were successfully printed into 3D porous hydrogel constructs with a thickness of more than 3 mm. Finally, 3D pre-vascularized cardiac constructs were successfully generated, indicating the efficacy of our strategy to engineer living tissues with complex vascular structures.

Keywords: Electrohydrodynamic bioprinting; Coaxial bioprinting; Vascularized tissues; Biofabrication; Core-sheath filaments

*Correspondence to: Jiankang He, State Key Laboratory for Manufacturing Systems Engineering, Xi'an Jiaotong University, Xi'an 710049, China; jiankanghe@mail.xjtu.edu.cn

Received: April 3, 2021; **Accepted:** May 14, 2021; **Published Online:** June 4, 2021

(This article belongs to the *Special Section*: *Bioprinting of 3D Functional Tissue Constructs*)

Citation: Mao M, Liang H, He J, *et al*., 2021, Coaxial Electrohydrodynamic Bioprinting of Pre-vascularized Cell-laden Constructs for Tissue Engineering. *Int J Bioprint*, 7(3):362. http://doi.org/10.18063/ijb.v7i3.362

1. Introduction

One of the most challenging problems in the tissue engineering area is to fabricate functional vasculature within the three-dimensional (3D) engineered tissue that provides enough nutrition and oxygen to the cells and transports the byproducts[1]. Cellular viability and function will be compromised, and necrosis may further occur without a capillary network within a few hundred microns of cells[2,3]. Thus, many approaches such as microreplication, photolithography, and sacrificial molding have been proposed to organize the endothelial cells in the spatially predefined organization, with an attempt to build microvessels within the cell-laden constructs[4-8]. It has been demonstrated that the endothelial cells in the spatially predefined organization can significantly improve the speed and extent of the vascularization after implantation, compared to that in a random distribution[9,10]. However, these engineering methods could only be used to fabricate constructs with relatively simple architectures and homogeneous cell-laden matrices, which make them difficult to recapitulate the intricate 3D structure and composition of natural tissues[11,12].

3D printing, mainly including the inkjet[13], extrusion[14], and vat polymerization-based processes[13-15], has evolved as a prevalent technology for producing 3D living tissue constructs with excellent controllability of geometrical shapes and complex microscale architectures. Especially, the inkjet or extrusion-based bioprinting approaches have been extensively explored over the past decade for creating 3D vascularized, heterogeneous cell-laden tissue constructs, owing to their remarkable advantages in wide suitability to various cell-laden bioinks and controllable positioning of the multicellular organization on demand[16-18]. However, as a consequence of the jetting or extrusion process through the printing nozzle, the cells would experience mechanical shear force inevitably, which has a negative effect on cell viability[19,20]. As smaller nozzles were usually employed to improve the printing resolution, the cell viability would further be challenged and clogging might occur when the viscous hydrogel was printed.

Electrohydrodynamic (EHD) printing, with inherent advantages in generating micro/nanoscale droplets or filaments, was recently explored to process cells-laden hydrogel for fabricating functional tissue constructs with high resolution and cell viability[21,22]. It is a novel hybrid inkjet printing combined with the electrospinning technique. When the electric field was applied on the printing nozzle, the bioink would be jetted out and the cells would experience a very low electrical current which would not cause notable damage to the cell integration, viability, and proliferation[23-25]. Since it was the electric force that pulled the bioink through the nozzle, the EHD cell printing process enabled to reduce the damage of shear stress on the printed cells which contributed to relatively high cell viability[26]. However, the nozzle-to-collector distance in these studies was over 600 μm to decrease the effect of high voltage on cell viability, and the size of the EHD-printed hydrogel filaments was larger than 200 μm[27,28]. To further improve the printing resolution, our group recently developed a novel EHD cell printing process by utilizing an insulating material to replace the conventional conductive or semiconductive material as the collecting substrate, which significantly reduced the electrical current on the bioink to microamperes (<10 μA)[29]. The feature size of the resultant hydrogel filament could be smaller than 100 μm while the cell viability was as high as 95%, implicating a potential strategy to build high-resolution living tissues. One limitation of this EHD cell printing process is that the height of the EHD-printed cell/hydrogel constructs was smaller than 145 μm, which resulted from the limited diffusion of calcium ions from the collecting substrate of agarose hydrogel to the deposited alginate filaments for crosslinking.

In this study, we integrated a coaxial nozzle into our house-made EHD cell printing system and explored its ability to fabricate thick pre-vascularized cell-laden constructs. When the collagen solution supplemented with calcium chloride ($CaCl_2$) in the inner layer and the alginate solution in the outer layer was pulled out of the coaxial nozzle by the electric force, instant crosslinking occurred when these bioink solutions met to form the core-sheath filaments. The width of the core and sheath hydrogel lines could be well modulated by changing the printing parameters such as the feeding rate of collagen solution and alginate solution as well as the moving speed of the substrate platform. Endothelialized lumen structure gradually formed along with the interface between the core and sheath lines when the endothelial cells were encapsulated into collagen solution as the inner-layer bioink. 3D porous hydrogel constructs with a thickness of more than 3 mm were successfully printed. As a concept of the study, we encapsulated endothelial cells and H9C2 cells into two layers of the coaxial nozzle, respectively, and successfully fabricated 3D pre-vascularized cardiac constructs.

2. Materials and methods

2.1. Materials and bioinks

Type I collagen derived from rat tail was prepared followed by previously described protocols and stored at 4°C. $CaCl_2$ and sodium hydroxide (NaOH) powder were purchased from Aladdin (Shanghai, China). Agarose powder with low melting temperature (87–89°C) was bought from Biowest (Spain). Alginate solution with a viscosity of 2000 mPa·S was prepared by dissolving alginate powder (Sigma, United Kingdom) into the cell culture medium with 10% (w/v) fetal bovine serum and 1% (w/v) antibiotic/antimycotic. 0.1 mol/L NaOH solution was prepared by dissolving NaOH powder into phosphate buffer saline (PBS) at room temperature. 3% (w/v) $CaCl_2$ solution was prepared by dissolving $CaCl_2$ powder into tris-buffered saline (TBS) at room temperature. 2% (w/v) flat agarose hydrogel was prepared by casting the boiling agarose solution with 3% (w/v) $CaCl_2$ into a petri dish at room temperature. Before the printing process, the pH of the collagen solution was adjusted to 7.2-7.6. GFP expressing human umbilical vein endothelial cells (GFP-HUVEC; ATCC, USA) and embryonic rat cardiomyocytes (H9C2; ATCC, USA) labeled with red cell tracker (Invitrogen, cat. no. C34552) were cultured in Dulbecco's Modified Eagle Medium (DMEM, Thermo) for printing cell-laden constructs.

2.2. EHD bioprinting setup

The EHD bioprinting setup is mainly composed of three key components: A high precision X-Y-Z moving stage (Xiamen Heidelstar, China), a voltage generator with high voltage (ZGF-30/5, Welldone, Shanghai, China), and a precision syringe pump system (TJ-2A, Longer Pump, Baoding, China). The coaxial printing nozzle (19G/26G) is mounted onto the Z-axis and connected with the high

voltage generator. The sheath and core layer of the coaxial nozzle is fed with alginate solution and collagen/$CaCl_2$ solution, respectively, by high-resolution syringes.

2.3. EHD bioprinting process

The process parameters of the applied voltage and nozzle-to-collector distance were fixed at 4.5 kV, 3.5 mm, 300 μm according to our previous studies[30]. When the high voltage syringe pumps run, alginate and collagen/$CaCl_2$ solution was simultaneously fed into the coaxial nozzle. Alginate was immediately cross-linked by the $CaCl_2$ solution when they met in the nozzle head. During the EHD bioprinting process, the printing room temperature should be lower than 16°C to avoid collagen solution gelling. After printing, the constructs were put into the cell culture incubator set at 37°C for 10 min for collagen solution gelling.

2.4. Optimization of EHD printing process parameters

The effects of the feeding rate of alginate and collagen solution and the moving speed of stage on the width of the printed core-sheath filaments were investigated when the applied voltage, the distance between nozzle and collecting substrate were fixed at 4.5 kV and 300 μm, respectively. Green fluorescent particles (Lumisphere, BaseLine, China) were added to the collagen solution to distinguish the core line from the sheath line in the hydrogel filaments. The bright-field and fluorescent images of the printed filaments were captured with an inverted fluorescence microscope (ECLIPSE Ti, Nikon, Japan), which were utilized to measure the size of the core line and sheath line.

2.5. Characterization of the lattice hydrogel with core-sheath filaments

A single layer of complex lattice hydrogel with core-sheath filaments was printed. To show the distribution of collagen and alginate hydrogel in the electrohydrodynamically printed core-sheath filaments, red and green fluorescent particles were added into the alginate and collagen solution, respectively. Hollow filaments were printed by replacing collagen solution with 3% (w/v) $CaCl_2$ solution. The fluorescent cross-section images of the printed hollow filaments were reconstructed using confocal microscope (Nikon, Japan). To evaluate the perfusability of the lattice hydrogel with hollow filaments, a syringe was connected to the opening of the hollow filament and a blue dye solution was injected; the process was recorded by a commercial camera.

2.6. Cell culture within the core-sheath filaments

The inner-layer bioink was prepared with GFP-HUVECs, collagen, and $CaCl_2$ at the final concentration of 2×10^6/mL, 0.3% (w/v) and 3% (w/v). The outer-layer bioink was 0.3% (w/v) pure alginate solution. Cellular morphology and distribution after different days in culture were characterized with an inverted fluorescence microscope and confocal microscope. The endothelialized filaments after 14 days in culture were captured using the digital camera (Nikon, Japan).

2.7. Fabrication of 3D hydrogel constructs

The EHD printing strategy was also employed to fabricate 3D complex lattice hydrogel by precisely stacking the filaments in a layer-by-layer manner. In this study, the macro/microscopic images of the 3D hydrogel constructs were captured with a digital camera and optical microscope. A confocal laser scanning microscope (OLS4000, Olympus, USA) was used to rebuild the 3D profiles of the printed constructs, which were used to quantify the height of constructs with different layers. The printed constructs with 5 layers were further freeze-dried in a lyophilizer (FD-1A-50, Biocool, Beijing, China) for 3 days. The microstructures were observed with a scanning electron microscope (SEM, SU8010, Hitachi, Japan).

2.8. Fabrication and characterization of cell-laden 3D constructs

To fabricate pre-vascularized 3D lattice constructs, the inner-layer bioink was prepared with GFP-HUVECs, collagen, and $CaCl_2$ at the final concentration of 2×10^6/mL, 0.3% (w/v) and 3% (w/v). The outer-layer bioink was 0.3% (w/v) pure alginate solution or 0.3% (w/v) alginate solution laden with red H9C2 cells at the final concentration of 2×10^6/mL. The bioprinted lattice constructs were cultured statically for different days. The proliferation of the printed cells was quantified using CCK-8 assay (Dojindo Molecular Technologies) on the culturing day of 1, 4, and 7. The cell viability was quantified by performing Live/Dead assay (Thermo Fisher Scientific).

2.9. Statistical analysis

All quantitative results were presented as mean ±standard deviation. Statistical significance was determined using one-way analysis of variance (ANOVA) followed by Tukey *post-hoc* test for multiple comparisons using SPSS statistical software. The differences were considered statistically significant if the p-value was <0.05 (*).

3. Results and discussion

3.1. EHD bioprinting of core-sheath hydrogel filaments

Figure 1 shows the EHD printing strategy integrated with a coaxial nozzle for fabricating the thick vascularized construct, assembled by the cross-linked core-sheath filaments. As illustrated in our previous study, an insulating

petri dish filled with 2% (w/v) agarose hydrogel was placed on the grounded stage as the collecting substrate to avoid the high electric current during the EHD printing process. The alginate and collagen/$CaCl_2$ solution were respectively controlled by two high-precision syringe pumps and loaded into the outer layer and inner layer of the coaxial nozzle. When the high voltage was applied, alginate solution and collagen/$CaCl_2$ solution would be pulled out of the coaxial nozzle simultaneously and the alginate solution would be instantly cross-linked by the calcium ions, resulting in core-sheath filaments deposited onto the collecting substrate under the control of the user-specific design. Multiple layers of constructs could be further printed by precisely stacking the core-sheath filaments in a layer-by-layer manner.

We then studied the effect of process parameters (feeding rate of alginate and collagen, moving speed of the printing stage) on the size of core and sheath within EHD printed filaments. Alginate solution and collagen/CaCl2/green fluorescent particles solution were loaded into the outer and inner layers of the coaxial nozzle, respectively. The size of the core line was characterized as the width of the bands with green fluorescent particles through the fluorescent images, while the size of the sheath line, defined as the external width of the filament, was measured in the same region through the bright-field images. **Figure 2A-E**

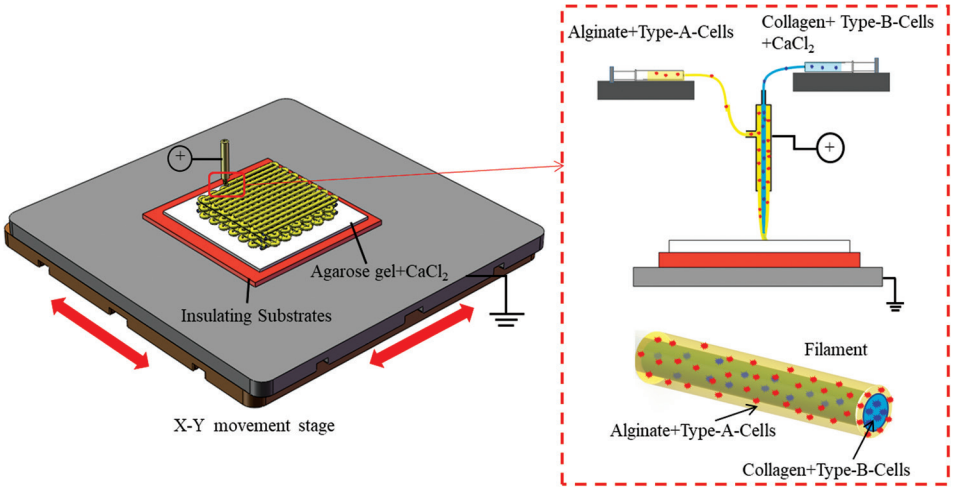

Figure 1. Schematic of EHD bioprinting strategy of core-sheath hydrogel filaments for generating cell-laden constructs.

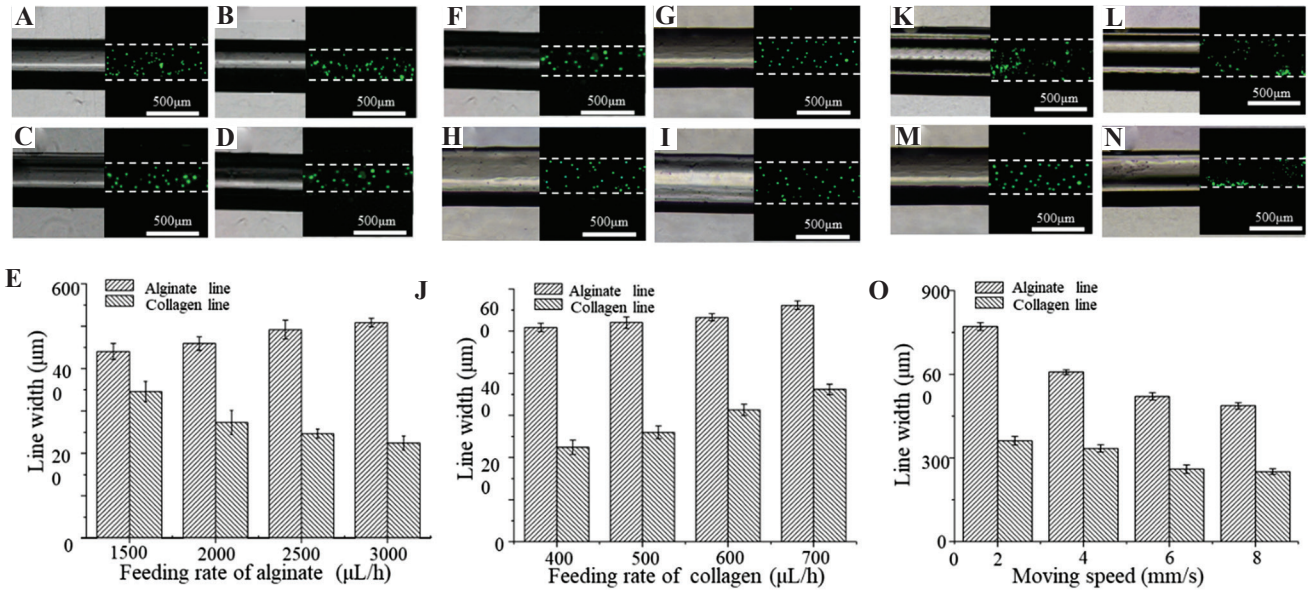

Figure 2. The effect of process parameters on the width of the EHD-bioprinted filaments. (A-E) The morphology and width of the core and sheath lines in the filaments as alginate feeding rate changed from 1500 μL/h to 3000 μL/h. (D-G) The morphology and width of the core and sheath lines in the filaments as collagen solution changed from 400 μL/h to 700 μL/h. (K-O) The morphology and width of the core and sheath lines in the filaments as moving speed changed from 2 mm/s to 8 mm/s.

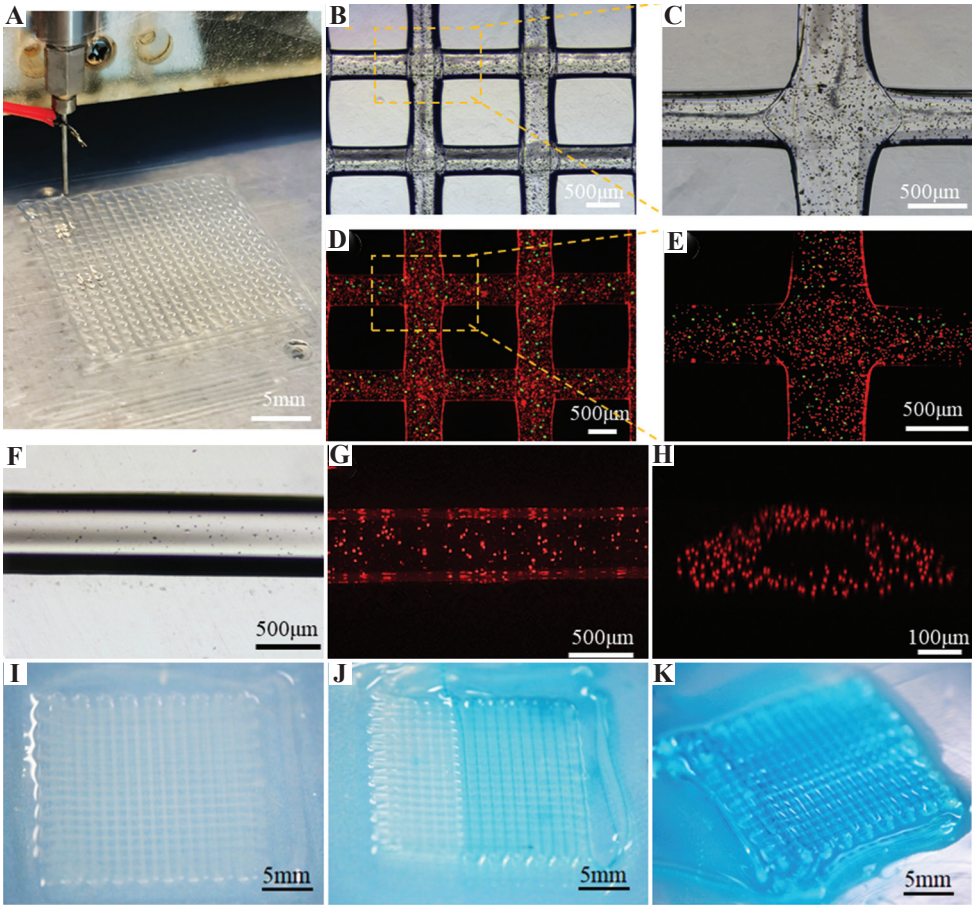

Figure 3. EHD bioprinting of lattice hydrogel with the core-sheath filaments. (A-C) The macroscopical and microscopical morphology of the lattice structures. (D and E) The core-sheath hydrogel filaments with green microbeads in the core line and red microbeads in the sheath line. The bright-field image (F) and fluorescent image (G) of the hollow hydrogel filament. (H) The cross-section of the 3D reconstructed models of hollow hydrogel filament. (I-K) Dye perfusion through the hollow filaments.

shows the effect of the feeding rate of alginate solution on the width of the EHD printed core-sheath filaments when the feeding rate of collagen solution and moving speed of stage were fixed at 400 μL/h and 6mm/s. It was found that the sheath-line width of the alginate filaments increased from 440 ± 18.79 μm to 508.75 ± 10.08 μm and the core-line width of the collagen filaments gradually decreased from 346 ± 23.63 μm to 224.5 ± 16.82 μm when the feeding rate of alginate of the solution changed from 1500 μL/h to 3000 μL/h (**Figure 2E**). **Figure 2F-I** shows the effect of the feeding rate of collagen solution on the width of the EHD printed core-sheath filaments when the feeding rate of alginate solution and moving speed fixed at 3000 μL/h and 6 mm/s. It was found that the sheath-line width of the alginate filaments increased from 508.75 ± 10.08 μm to 561.42 ± 10.14 μm and the core-line width of the collagen filaments increased from 224.5 ± 16.81 μm to 361.57 ± 12.37 μm when the feeding rate of collagen solution increased from 400 μL/h to 700 μL/h (**Figure 2G**). We then studied the effect of the moving speed of the printing stage on the width of the EHD printed core-sheath filaments when the feeding rate of alginate and collagen solution was fixed at 3000 μL/h and 500 μL/h (**Figure 2K-N**). It was found that when the moving speed of the printing stage increased from 2 mm/s to 8 mm/s, the width of the sheath and core line decreased from 771.5 μm to 486.86 μm and from 361.5 μm to 250.8 μm, respectively (**Figure 2O**). These results indicate that the size of the core and sheath within the EHD printed filaments could be modulated independently by changing the feeding rate of the solution in the outer and inner layers of the coaxial nozzle, while the higher moving speed of the printing stage leads to thinner sheath-core hydrogel filament. In the subsequent EHD bioprinting process, the feeding rate of alginate and collagen, as well as the moving speed of the stage, was set as 3000 μL/h, 500 μL/h, and 6 mm/s.

3.2. EHD bioprinting of the lattice hydrogel with core-sheath filaments

The presented EHD-bioprinting method was further employed to fabricate complex lattice hydrogel with core-

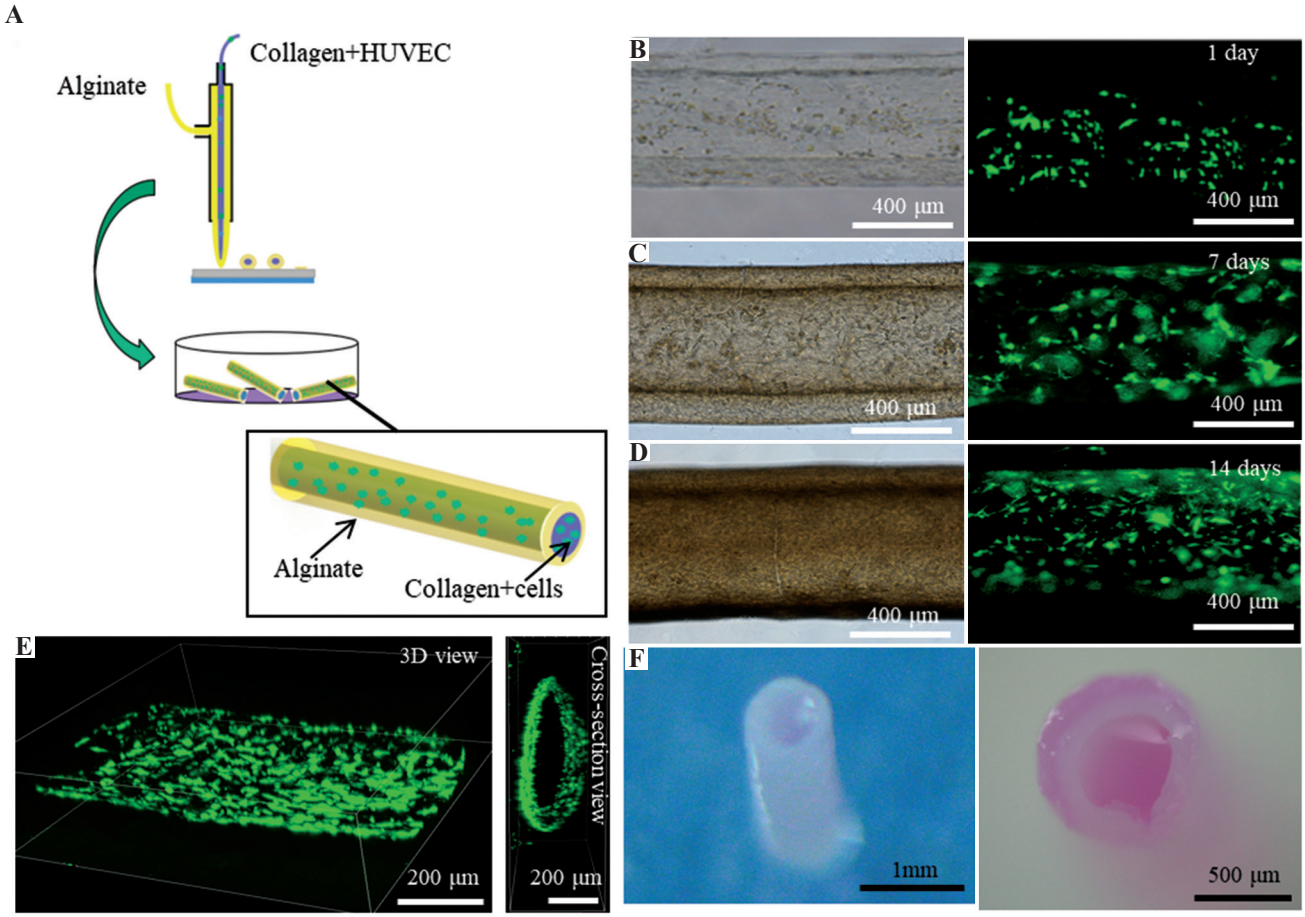

Figure 4. The growth of HUVECs in the core-sheath filaments. (A) The schematic of printing core-sheath filaments laden with HUVECs in the core collagen line. (B-D) The morphology of HUVECs within the filaments during 14 days in static culture. (E) The 3D structure of the formed circular vessel within the filament. (F) The morphology of the core-sheath filament after 14 days in culture.

sheath filaments (**Figure 3A**). Alginate/red fluorescent particles solution and collagen/$CaCl_2$/green fluorescent particles solution were loaded into the outer and inner layer of the coaxial nozzle, respectively. The EHD printed core-sheath filaments maintained excellent morphology and architecture during the printing of complex lattice structures, indicating its potential to fabricate 3D porous constructs for tissue engineering (**Figure 3B and C**). The green fluorescent particles mainly remained in the center of the red fluorescent area, indicating the well-formed core-sheath hydrogel filament with collagen core encapsulated by the alginate sheath without leakage (**Figure 3D and E**).

The collagen/$CaCl_2$/green fluorescent particles solution was replaced by the pure $CaCl_2$ solution to print the hollow hydrogel filaments with perfusable lumen structures. It was found that the printed alginate solution was cross-linked by the $CaCl_2$ solution to form a table hollow hydrogel filament (**Figure 3F**). Red fluorescent particles were uniformly distributed within the ring wall of the hollow filament and the lumen structure was well maintained, as shown in the top-view fluorescent image (**Figure 3G**) and cross-section of the 3D confocal profile (**Figure 3H**). This result demonstrated that the crosslinking between alginate solution and calcium ions occurred instantly when they met and the encapsulated cells would also be maintained uniformly during the printing process in future work. The perfusability of the lattice hydrogel assembled by the hollow filaments was then evaluated by a dye injection test. The blue dye solution could circulate rapidly through the hollow filaments with the predefined lattice pattern, suggesting that this printed lattice hydrogel with lumen filaments is well perfusable (**Figure 3I-K**).

3.3. Fabrication and characterization of the endothelialized lumen structure in the core-sheath filaments

To fabricate the endothelialized filaments, GFP-HUVECs were added into collagen/$CaCl_2$ solution as the inner-layer

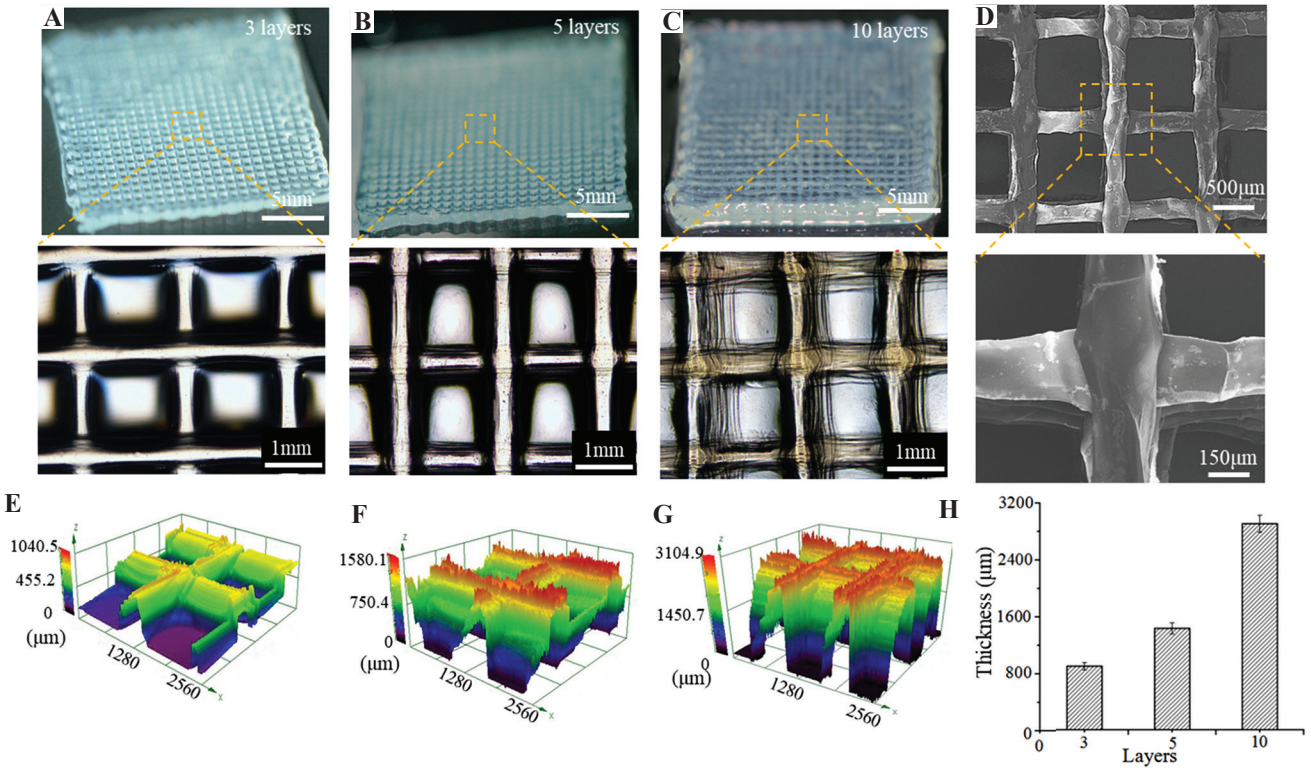

Figure 5. 3D porous hydrogel constructs with different layer numbers. (A-C) Macroscopical and microscopical images of the constructs with 3, 5, and 10 layers. (D) SEM images of the constructs with 5 layers after freeze-drying. (E-G) The 3D confocal profiles of the constructs. (H) Quantification of the thickness of the constructs.

bioink for EHD-bioprinting (**Figure 4A**). **Figure 4B-D** shows the morphology and distribution of HUVECs encapsulated in collagen gelation during 14 days in culture. It was found that the HUVECs maintained high viability and began to spread within the inner collagen layer after 2 days in culture. There was then a notable cell proliferation after 14 days in culture. It was interesting to observe that the cells migrated into the interface between the core and sheath hydrogel and formed a circular vessel along the filament instead of randomly distributing in the core (**Figure 4E**). This might be owing to the swelling and degradation of the collagen gel during the long culturing time, allowing for the movement of cells within the hydrogel filament. The endothelialized hydrogel filaments maintained good morphology during 14 days in culture (**Figure 4F**).

3.4. EHD-bioprinting of 3D porous hydrogel constructs

To investigate the feasibility of generating 3D porous hydrogel constructs, multilayer core-sheath filaments were further printed into lattice structures. **Figure 5A-C** shows the photo images and the corresponding microscopical images of the printed constructs with 3, 5, and 10 layers, indicating that the assembled core-sheath filaments maintained good line feature, predefined layout, and lattice structures during the printing process for all the groups. A substantial increase in the thickness of the constructs could be observed with more layers. **Figure 5D** shows SEM images of the printed lattice hydrogel constructs with 5 layers. It can be found that the neighboring layers were tightly merged, which still maintained structural integrity after freeze-drying. The diameter of the freeze-dried filaments was smaller than the printed hydrogel filaments due to water loss and shrinking during the freeze-drying process. The thickness of the printed constructs with different layers was characterized by 3D confocal profiles (**Figure 5E-G**). The measured thickness of the printed constructs increased from 894.35 ± 41.50 μm to 2893.85 ± 92.60 μm as the layer number increased from 3 to 10 (**Figure 5H**). The average height of each layer was about 290.75 ± 12.22 μm, which indicated that the printed core-sheath filaments in each layer could maintain good morphology and relatively stable thickness. These results indicated that this coaxial EHD bioprinting

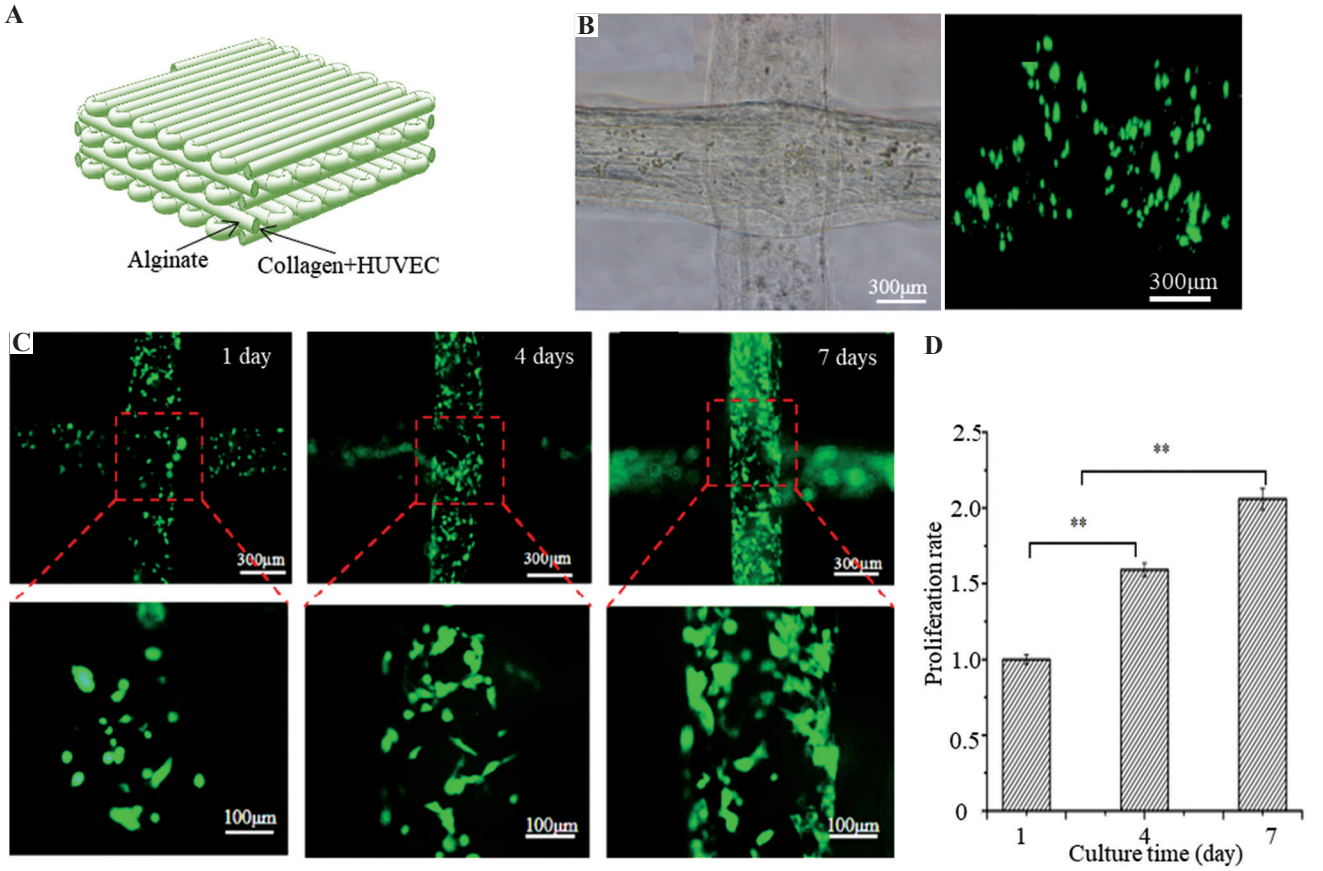

Figure 6. Engineering 3D vasculature within the lattice hydrogel. (A) The schematic of the hydrogel constructs laden with HUVECs within the core collagen bioink. (B) The bright-field image and 3D fluorescent profiles of the 3D lattice hydrogel laden with HUVECs after 3 hours in culture. (C) The growth of HUVECs within the lattices during 7 days in culture. (D) The proliferation of cells within 3D lattice hydrogel during 7 days in culture.

strategy might be employed to fabricate cell-laden 3D constructs for tissue engineering.

3.4. EHD bioprinting of pre-vascularized cell-laden constructs

Alginate and collagen/$CaCl_2$/HUVECs solution was utilized as the outer and inner-layer bioink, respectively, for EHD-bioprinting of pre-vascularized 3D lattice constructs (**Figure 6A**). **Figure 6B** shows the bioprinted lattice hydrogel with stable structures and the 3D fluorescent profiles of HUVECs encapsulated in the lattice hydrogel after 3 hours in culture. The spreading and proliferation of the encapsulated HUVECs within the filaments could be obviously observed during the static culture (**Figure 6C**). The constructs still maintained their morphological and structural features while the cell number was doubled after 7 days (**Figure 6D**), which demonstrated that the printed 3D porous lattice structures were beneficial to the mass transfer of the encapsulated cells. The results of live-dead staining indicated that the cell viability of the constructs increased from 92.5% to 96.3% after 7 days in culture. All these results indicated that the printed porous lattice hydrogel had a potential for engineering 3D vascularized constructs with predefined structures in the future.

As a proof of concept study we sought to employ the coaxial EHD bioprinting strategy for engineering pre-vascularized cardiac constructs by encapsulating H9C2 cells, a cardiac cell line, into alginate solution as the outer-layer bioink. **Figure 7B** shows the optical and fluorescence images of the cell-laden constructs after 1 day in culture, showing that HUVEC cells (green) were surrounded uniformly by the H9C2 cells (red) in 3D constructs. After 2 days in culture, all the cells maintained well viability and the HUVEC cells began to spread and became oriented along the filaments, showing that the coaxial EHD bioprinting strategy has the potential of engineering pre-vascularized cell-laden constructs.

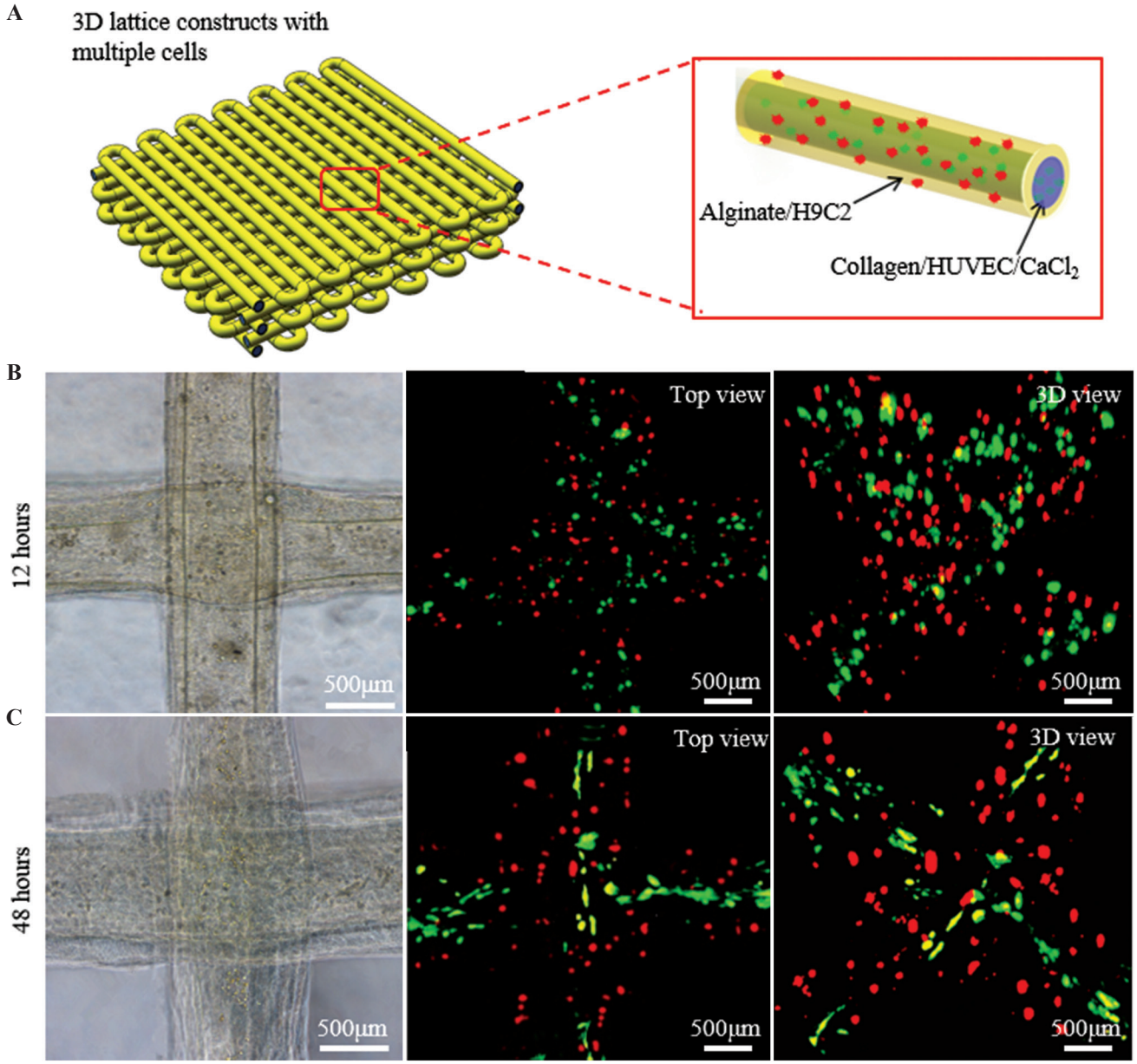

Figure 7. EHD bioprinting of pre-vascularized cardiac constructs. (A) The schematic of the hydrogel constructs laden with HUVECs and H9C2 cells within the core collagen and sheath alginate bioinks, respectively. (B and C) The morphology of the lattice structures and the growth of HUVECs (green) and H9C2 cells (red) within the hydrogel constructs during 48 h in culture.

4. Conclusion

In this study, a coaxial nozzle was introduced into the EHD bioprinting system to fabricate pre-vascularized constructs, which were assembled by the printed core-sheath hydrogel filaments. To stably print the filaments, some process parameters, such as feeding rate of alginate and collagen solution, and moving speed of stage were investigated. HUVECs were added into collagen solution as inner-layer bioink in the coaxial nozzle to generate endothelialized filaments. During cell culture, the cells gradually spread and migrated to the interface between the core collagen line and sheath alginate line and formed a biomimetic lumen vessel structure. 3D constructs with 3, 5, and 10 layers were printed, demonstrating that the hydrogel filaments in each layer maintained their morphology and enabled the formation of thick porous hydrogel construct of more than 3 mm. 3D constructs with HUVECs encapsulated into the core collagen filaments were electrohydrodynamically printed. The cells not only maintained high viability but also spread and proliferated during 7 days in static culture, indicating that the porous structures were beneficial to the nutrition

supply. Finally, GFP-HUVECs and H9C2 cells were mixed with inner-layer collagen and out-layer alginate solution, respectively, to fabricate 3D pre-vascularized cardiac constructs. It was noted that the HUVECs encapsulated in collagen gel were able to spread and align along the filaments surrounded by the H9C2 cells in the 3D constructs. These results demonstrate that this coaxial EHD bioprinting method has great potential to fabricate complex 3D tissues or organs with vascular network.

Acknowledgments

This work was financially supported by the National Key Research and Development Program of China (2018YFA0703000), the Key Research Project of Shaanxi Province (2020GXLH-Y-021), Guangdong Basic and Applied Basic Research Foundation (2020B1515130002), The Youth Innovation Team of Shaanxi Universities, and the Fundamental Research Funds for the Central Universities.

Conflict of interest

No conflict of interest were reported by the authors.

Author contributions

M.M. and H.L. designed the overall experimental plan and performed experiments. M.M. wrote the manuscript with support from H.L. and J.H., and co-authors A.K., Y.Z., L.W., and X.L. involved in the investigation and analysis of results. J.H. and D.L. supervised the project and conceived the original idea.

References

1. Zhu W, Qu X, Zhu J, *et al.*, 2017, Direct 3D Bioprinting of Prevascularized Tissue Constructs with Complex Microarchitecture. *Biomaterials*, 124:106–15. https://doi.org/10.1016/j.biomaterials.2017.01.042
2. Baranski JD, Chaturvedi RR, Stevens KR, *et al.*, 2013, Geometric Control of Vascular Networks to Enhance Engineered Tissue Integration and Function. *Proc Natl Acad Sci U S A*, 110:7586–91. https://doi.org/10.1073/pnas.1217796110
3. Bertassoni LE, Cecconi M, Manoharan V, *et al.*, 2014, Hydrogel Bioprinted Microchannel Networks for Vascularization of Tissue Engineering Constructs. *Lab Chip*, 14:2202–11. https://doi.org/10.1039/c4lc00030g
4. Qiu Y, Ahn B, Sakurai Y, *et al.*, 2018, Microvasculature-on-a-chip for the Long-term Study of Endothelial Barrier Dysfunction and Microvascular Obstruction in Disease. *Nat Biomed Eng*, 2:453–63. https://doi.org/10.1038/s41551-018-0224-z
5. Miller JS, Stevens KR, Yang MT, *et al.*, 2012, Rapid Casting of Patterned Vascular Networks for Perfusable Engineered Three-dimensional Tissues. *Nat Mater*, 11:768. https://doi.org/10.1038/NMAT3357
6. Mao M, Bei HP, Lam CH, *et al.*, 2020, Human-on-Leaf-Chip: A Biomimetic Vascular System Integrated with Chamber-Specific Organs. *Small*, 16:2000546. https://doi.org/10.1002/smll.202000546
7. He J, Mao M, Liu Y, *et al.*, 2013, Fabrication of Nature-Inspired Microfluidic Network for Perfusable Tissue Constructs. *Adv Healthc Mater*, 2:1108–13. https://doi.org/10.1002/adhm.201200404
8. Lenoir L, Segonds F, Nguyen KA, *et al.*, 2019, A Methodology to Develop a Vascular Geometry for *In Vitro* Cell Culture Using Additive Manufacturing. *Int J Bioprint*, 5:238. https://doi.org/10.18063/ijb.v5i2.238
9. Mirabella T, MacArthur JW, Cheng D, *et al.*, 3D-printed Vascular Networks Direct Therapeutic Angiogenesis in Ischaemia. *Nat Biomed Eng*, 1:0083. https://doi.org/10.1038/s41551-017-0083
10. Yao R, Alkhawtani AY, Chen R, *et al.*, 2019, Rapid and Efficient *In Vivo* Angiogenesis Directed by Electro-assisted Bioprinting of Alginate/Collagen Microspheres with Human Umbilical Vein Endothelial Cell Coating Layer. *Int J Bioprint*, 5:194. https://doi.org/10.18063/ijb.v5i2.1.194
11. Hasan A, Paul A, Vrana NE, *et al.*, 2014, Microfluidic Techniques for Development of 3D Vascularized Tissue. *Biomaterials*, 35:7308–25. https://doi.org/10.1016/j.biomaterials.2014.04.091
12. Ng WL, Chua CK, Shen YF, 2019, Print Me An Organ! Why We Are Not There Yet. *Prog Polym Sci*, 97:101145. https://doi.org/10.1016/j.progpolymsci.2019.101145
13. Li X, Liu B, Pei B, *et al.*, 2020, Inkjet Bioprinting of Biomaterials. *Chem Rev*, 120:10793–833. https://doi.org/10.1021/acs.chemrev.0c00008
14. Jiang T, Munguia-Lopez JG, Flores-Torres S, *et al.*, 2019, Extrusion Bioprinting of Soft Materials: An Emerging Technique for Biological Model Fabrication. *Appl Phys Rev*, 6:30. https://doi.org/10.1063/1.5059393
15. Ng WL, Lee JM, Zhou M, *et al.*, 2020, Vat Polymerization-based Bioprinting-Process, Materials, Applications and Regulatory Challenges. *Biofabrication*, 12:022001. https://doi.org/10.1088/1758-5090/ab6034
16. Kolesky DB, Homan KA, Skylar-Scott MA, *et al.*, 2016,

Three-dimensional Bioprinting of Thick Vascularized Tissues. *Proc Natl Acad Sci*, 113:3179–84. https://doi.org/10.1073/pnas.1521342113

17. Kolesky DB, Truby RL, Gladman AS, *et al.*, 2014, 3D Bioprinting of Vascularized, Heterogeneous Cell-laden Tissue Constructs. *Adv Mater*, 26:3124. https://doi.org/10.1002/adma.201305506
18. Feng F, He J, Li J, *et al.*, 2019, Multicomponent Bioprinting of Heterogeneous Hydrogel Constructs Based on Microfluidic Printheads. *Int J Bioprint*, 5:202. https://doi.org/10.18063/ijb.v5i2.202
19. Kang HW, Lee SJ, Ko IK, *et al.*, 2016, A 3D Bioprinting System to Produce Human-scale Tissue Constructs with Structural Integrity. *Nat Biotechnol*, 34:312–9. https://doi.org/10.1038/nbt.3413
20. Murphy SV, Atala A, 2014, 3D Bioprinting of Tissues and Organs. *Nat Biotechnol*, 32:773. https://doi.org/10.1038/nbt.2958
21. He J, Zhang B, Li Z, *et al.*, 2020, High-resolution Electrohydrodynamic Bioprinting: A New Biofabrication Strategy for Biomimetic Micro/Nanoscale Architectures and Living Tissue Constructs. *Biofabrication*, 12:042002. https://doi.org/10.1088/1758-5090/aba1fa
22. Huo H, Liu F, Luo Y, *et al.*, 2020, Triboelectric Nanogenerators for Electro-assisted Cell Printing. *Nano Energy*, 67:104150. https://doi.org/10.1016/j.nanoen.2019.104150
23. Gasperini L, Maniglio D, Motta A, *et al.*, An Electrohydrodynamic Bioprinter for Alginate Hydrogels Containing Living Cells. *Tissue Eng Part C Methods*, 21:123–32. https://doi.org/10.1089/ten.tec.2014.0149
24. Workman VL, Tezera LB, Elkington PT, *et al.*, 2014, Controlled Generation of Microspheres Incorporating Extracellular Matrix Fibrils for Three-Dimensional Cell Culture. *Adv Funct Mater*, 24:2648–57. https://doi.org/10.1002/adfm.201303891
25. Sampson SL, Saraiva L, Gustafsson K, *et al.*, Cell Electrospinning: An *In Vitro* and *In Vivo* Study. *Small*, 10:78–82. https://doi.org/10.1002/smll.201300804
26. Jayasinghe SN, Qureshi AN, Eagles PA, 2006, Electrohydrodynamic Jet Processing: An Advanced Electric-Field-Driven Jetting Phenomenon for Processing Living Cells. *Small*, 2:216–9. https://doi.org/10.1002/smll.200500291
27. Wang J, Huang R, Chen H, *et al.*, 2019, Personalized Single-Cell Encapsulation Using E-Jet 3D Printing with AC-Pulsed Modulation. *Macromol Mater Eng*, 304:1800776. https://doi.org/10.1002/mame.201800776
28. Yeo M, Ha J, Lee H, *et al.*, 2016, Fabrication of hASCs-laden Structures Using Extrusion-based Cell Printing Supplemented with an Electric Field. *Acta Biomater*, 38:33–43. https://doi.org/10.1016/j.actbio.2016.04.017
29. He J, Zhao X, Chang J, *et al.*, 2017, Microscale Electro-Hydrodynamic Cell Printing with High Viability. *Small*, 2017:1702626. https://doi.org/10.1002/smll.201702626
30. Liang HT, He JK, Chang JK, *et al.*, 2018, Coaxial Nozzle-assisted Electrohydrodynamic Printing for Microscale 3D Cell-laden Constructs. *Int J Bioprint*, 4:8. https://doi.org/10.18063/IJB.v4i1.127